

Cite this: *Chem. Sci.*, 2025, **16**, 6480

All publication charges for this article have been paid for by the Royal Society of Chemistry

Received 23rd January 2025
Accepted 6th March 2025

DOI: 10.1039/d5sc00605h
rsc.li/chemical-science

Introduction

Glycosylation, a universal modification found across all domains of life, leads to the formation of diverse glycoconjugates.¹ Glycoproteins, which are conjugates of protein molecules with one or more sugar units, exhibit remarkable structural and functional diversity and play pivotal roles in numerous biological processes.² Similarly, ribosomally synthesized and post-translationally modified peptide (RiPP) natural products are derived from ribosomally produced precursor peptides. These RiPPs undergo maturation through enzyme-catalyzed post-translational modifications (PTMs), facilitated by specific interactions between PTM enzymes and the leader and/or core regions of the precursor peptides.³ In contrast to the widespread occurrence of glycoproteins, glycosylation in RiPP biosynthesis is relatively rare.⁴

Among RiPPs, glycocins are the only class defined by glycosylation as their hallmark PTM, with 13 experimentally characterized members.⁵ Additionally, a few other RiPP members, including nine thiopeptides (across four series),^{6–13} two

lanthipeptides,^{14,15} and two homologous lasso peptides,¹⁶ have been reported to feature glycosylation.⁴ Compared to glycosylated RiPP natural products, the glycosyltransferases (GTs) responsible for RiPP glycosylation are even less characterized. Most characterized RiPP GTs originate from glycocin biosynthetic pathways,^{3,5} which are predicted to belong to the GT2 family.^{5,17,18} A defining feature of glycocin GTs is their ability to catalyze *S*-linked glycosylation at specific Cys residues within precursor peptides (Fig. 1A).^{5,18}

A few glycocins, such as thurandacin and glycocin F, exhibit both *S*- and *O*-glycosylation (at Ser or Thr), catalyzed by a single GT with broad chemoselectivity.^{5,18–23} These GTs demonstrate iterative glycosylation activity, with the *S*-glycosylation occurring first and more rapidly than the subsequent *O*-glycosylation.^{20,23} Generally, glycocin GTs act on linear precursor peptides as the first step in glycocin biosynthesis.

Three GTs (*Ap*-GT3, *Sr*-GT822, and *Per*S4) have been found to attach *L*-rhamnose or *D*-glucose to the 3-hydroxypyridine moiety of nosiheptide (Fig. 1B).^{7,13} Notably, *Sr*-GT822 was not found within a thiopeptide biosynthetic gene cluster (BGC) but was identified through biotransformation of nosiheptide using *Streptomyces* sp. 147326 and subsequent bioinformatic and enzymatic analysis.¹³

The class III lanthipeptide NAI-112 is modified with a rare deoxyhexose group attached to the N-1 of a Trp residue, alongside labionin and methylabionin motifs.¹⁴ The GT *Ap*-Ig was shown to perform single Trp-glycosylation after the formation of intact ring structures during NAI-112 biosynthesis, as demonstrated through *in vivo* co-expression studies

^aState Key Laboratory of Applied Organic Chemistry, College of Chemistry and Chemical Engineering, School of Pharmacy, Lanzhou University, Lanzhou 730000, People's Republic of China. E-mail: dongsh@lzu.edu.cn

^bAcademy of Plateau Science and Sustainability, Qinghai Normal University, Xining 810016, People's Republic of China

[†] Electronic supplementary information (ESI) available: Experimental procedures and supplementary figures and tables. See DOI: <https://doi.org/10.1039/d5sc00605h>

[‡] Contributed equally to this work.



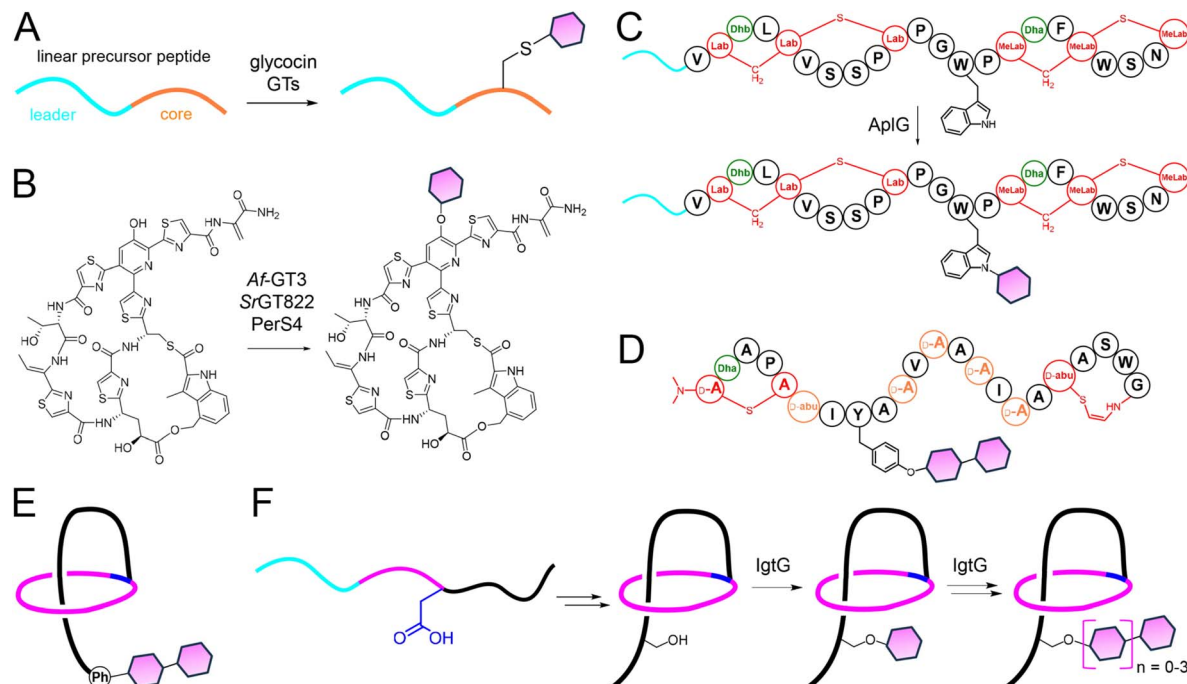


Fig. 1 Schematic depiction of representative glycosylated RiPPs and associated GTs. (A) Glycycin GTs catalyze glycosylation on linear precursor peptides. (B) Three GTs mediate glycosylation of the 3-hydroxypyridine moiety in nosiheptapeptide. (C) AplG catalyzes *N*-glycosylation of a Trp during NAI-112 biosynthesis. (D) The structure of cacaoidin features diglycosylation on a Tyr. (E) Pseudomycoidin exhibits diglycosylation on a phosphate group (Ph). (F) The biosynthesis of davasins involves the iterative action of GT IgtG on mature lasso peptides.

(Fig. 1C).²⁴ Cacaoidin, a class V lanthipeptide, features several unique PTMs, including diglycosylation on a Tyr residue, *N,N*-dimethyl lanthionine, aminobutyric acid, dehydroalanine, and aminovinyl-methyl-cysteine (Fig. 1D).¹⁵ The BGC of cacaoidin, identified and verified through bioinformatics and heterologous expression, encodes three GTs that are believed to cooperatively catalyze the attachment of two sugar moieties.^{15,25}

Glycosylated lasso peptides, pseudomycoidins, have been characterized as containing one or two hexose residues attached to a phosphate group linked to the C-terminal Ser (Fig. 1E).¹⁶ In the corresponding BGC, no obvious GT gene was identified. Instead, a nucleotidyltransferase, PsmN, was shown to be essential for mono- and diglycosylation, as demonstrated by heterologous expression of the *psm* genes in *E. coli*.¹⁶ However, the lack of observed *in vitro* catalytic activity raises questions about its true substrate—whether it acts on the phosphorylated linear peptide or the phosphorylated lasso peptide.¹⁶

Notably, only two classes of PTM enzymes have been proven to act on mature lasso peptides rather than their linear precursor peptides.^{26–28} The first class includes protein L-isopropyl aspartyl methyltransferase (PIMT) homologues,^{27,28} which exclusively catalyze aspartimide formation within the mature lasso structure. The second class involves GCN5-related *N*-acetyltransferases (GNATs), which iteratively and consecutively acylate two Lys residues within the loop and ring motifs of lasso peptides.²⁹

In this study, we report the discovery of a novel group of Ser-polyglycosylated lasso peptides from *S. davaonensis* JCM 4913. The corresponding *igt* BGC and a single GT, IgtG, responsible

for polyglycosylation, were identified through gene knockout and heterologous expression. *In vitro* assays using IgtG-expressing microsomes revealed an unprecedented catalytic function of IgtG, which iteratively glycosylates mature lasso peptides instead of their linear counterparts (Fig. 1F). This iterative glycosylation at a single residue of a lasso peptide represents a unique PTM, thereby expanding the catalytic diversity of the widely distributed GT enzyme superfamily.

Results and discussion

Discovery and characterization of polyglycosylated lasso peptides

To discover novel RiPPs, which often have larger molecular weights than other natural product families, matrix-assisted laser desorption/ionization time-of-flight mass spectrometry (MALDI-TOF MS) screening was performed on metabolites from in-house actinomycete cultures. The screening focused on a mass range between *m/z* 1000 and 2500. For the whole extract of *S. davaonensis* JCM 4913 grown in PTM medium, three prominent mass peaks were observed at *m/z* 1638.9, 1800.8, and 1963.2 (Fig. S1†). Similar peaks were also detected in samples from MB medium but were absent in samples from TSB, MD, YEME, or ISP2 media.

The PTM medium extract of *S. davaonensis* JCM 4913 was further analyzed by liquid chromatography high-resolution mass spectroscopy (LC-HRMS) (Fig. 2A). This analysis revealed a series of related mass peaks with $[M + 2H]^{2+}$ ions at 819.9677, 900.9941, 982.0209, 1063.0479, and 1144.0726 (Fig. 2B and S2†).

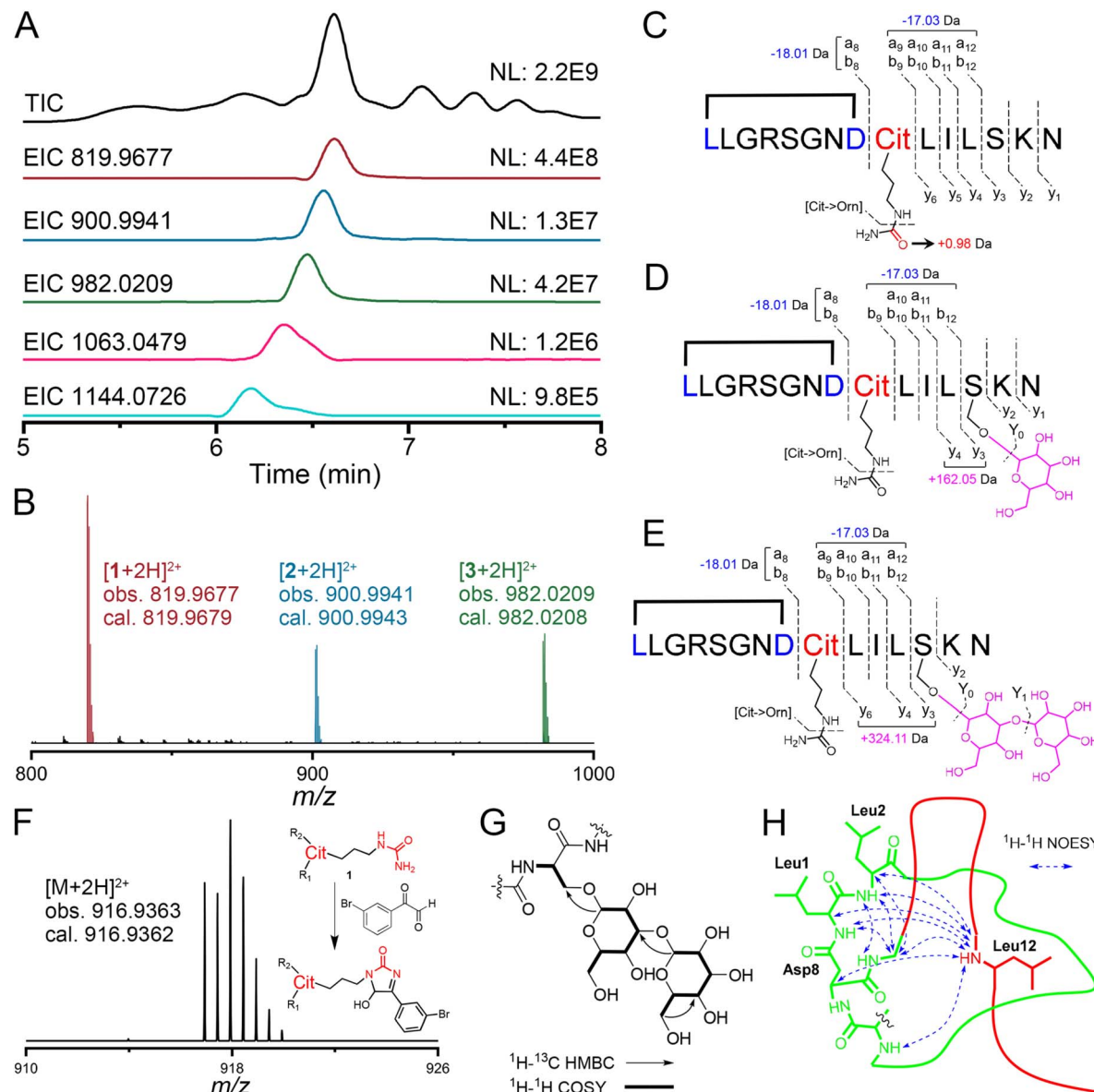


Fig. 2 Discovery and characterization of glycosylated lasso peptides. (A) LC-HRMS analysis of the *S. davaonensis* JCM 4913 extract. (B) HRMS spectra of 1–3. (C–E) HRMS/MS analysis of 1–3. Corresponding spectra are shown in Fig. S3–S5.† (F) HRMS spectrum of the adduct of 1 and 3-bromophenylglyoxal. (G) Key COSY and HMBC NMR correlations of the Ser-disaccharide region of 1. (H) Key NOESY NMR correlations between residues in the tail and ring regions of 1. The NMR spectra are shown in Fig. S6–S16.†

The successive differences of 162.05 Da between these peaks suggested the presence of homologous metabolites with varying glycosylation states.

The three most intense peaks, corresponding to compounds 1, 2, and 3 (designated as davasins A, B, and C), were subjected to tandem mass fragmentation analysis (Fig. 2C–E and S3–S5.†). The MS/MS spectra revealed shared large fragment ions (a₈ and b₈), indicative of a stable fragment structure, such as a peptidyl macrocycle. Detailed analysis of the b₉ and b₈ ion differences in the three spectra suggested the presence of a citrulline (Cit) residue at this position. Cit-containing lasso peptides have been previously reported,^{30,31} and their formation has been shown to result from the action of distally encoded peptidyl arginine deiminases that catalyze Arg deimination.³¹ Further analysis of

the MS/MS spectra identified mono- and diglycosylation modifications, both localized to a Ser residue.

Given the rarity of glycosylated RiPPs, particularly poly-glycosylated RiPPs (Fig. 1), we aimed to isolate the corresponding compounds by tracing their mass signals through the purification process. Using continuous chromatography, we successfully purified two compounds, 1 and 3, with observed masses of [M + 2H]²⁺ 819.9677 and 982.0209, respectively.

The presence of Cit in 1 was confirmed through derivatization with 3-bromophenylglyoxal, which selectively targets primary ureido groups.³¹ The derivatized product of 1 was detected, displaying a characteristic isotopic pattern of a Br atom in the HRMS spectrum (Fig. 2F).

The 1D- and 2D-NMR spectra of **1** and **3** were recorded (Tables S1–S4 and S6–S16†), enabling detailed characterization of individual residues and, most importantly, the identification of the linkage between the Ser side chain hydroxy group and the C1 of the glycosyl group (Fig. 2G and S17†). In the structure of **3**, the 1,3-glycosidic linkage between the two glycosyl groups was further confirmed through methylation analysis,³² which involved derivatisation, hydrolysis of the diglycosylated lasso peptide, and subsequent GC-MS analysis (Fig. S18†). Acid hydrolysis followed by derivatisation, HPLC analysis, and comparison with standard sugars derived by the same process revealed that the glycosyl groups in **3** consist of a mixture of L- and D-glucoses in a 1 : 3 ratio (Fig. S19†).³³ Finally, the lasso conformation of **1** and **3** was supported by ¹H-¹H NOESY signals, which revealed interactions between residues in the linear and ring motifs (Fig. 2H, S11 and S16†).

Compounds **1** and **3** were then evaluated for antibacterial and cytotoxic activity; however, no activity was observed up to a concentration of 50 μ M. Further biological screening is needed to assess the significance of the diglycosyl group.

IgtG is an iterative GT *in vivo*

Using the antiSMASH online server, a canonical lasso peptide BGC named *igt* was identified in the genome of *S. davaonensis*

JCM 4913, correlating with the structures of **1**–**3** (Fig. 3A and Table S5†).^{34,35} The precursor peptide IgtA was predicted to contain a core peptide sequence that perfectly matched the mass and NMR data. Alongside the lasso cyclase IgtC, the RIPP recognition element IgtB1, and the *trans*-glutaminase (protease) IgtB2, the *igt* BGC encodes IgtG, a putative bifunctional polysaccharide deacetylase/glycosyltransferase family 2 protein (domain architecture ID 11679047). IgtG was predicted to be a membrane protein with four transmembrane helices, as determined using the DeepTMHMM³⁶ server (Fig. S20†). The predicted *igt* genes align well with the structures of **1**–**3**.

The primary structural difference between the IgtA core peptide and **1**–**3** is the substitution of Arg9 in IgtA with Cit9 in the lasso peptides. A minor component structurally related to **1**, featuring Arg9 instead of Cit9 (compound **4**), was detected in the extract of *S. davaonensis* JCM 4913 (Fig. 3B), suggesting a correlation between the *igt* BGC and **1**–**3**. To confirm the essential role of the *igt* BGC in the biosynthesis of **1**–**3**, the *igtAC* gene fragment was deleted *via* homologous double-crossover using the pZDBlue plasmid.³⁷ The resulting *S. davaonensis* *ΔigtAC* strains completely lost the ability to produce **1**–**3** (Fig. S21†), confirming a direct link between the *igt* BGC and these lasso peptides.

To further investigate the role of IgtG, heterologous expression experiments were conducted with *igtABCD* and *igtABCDG*

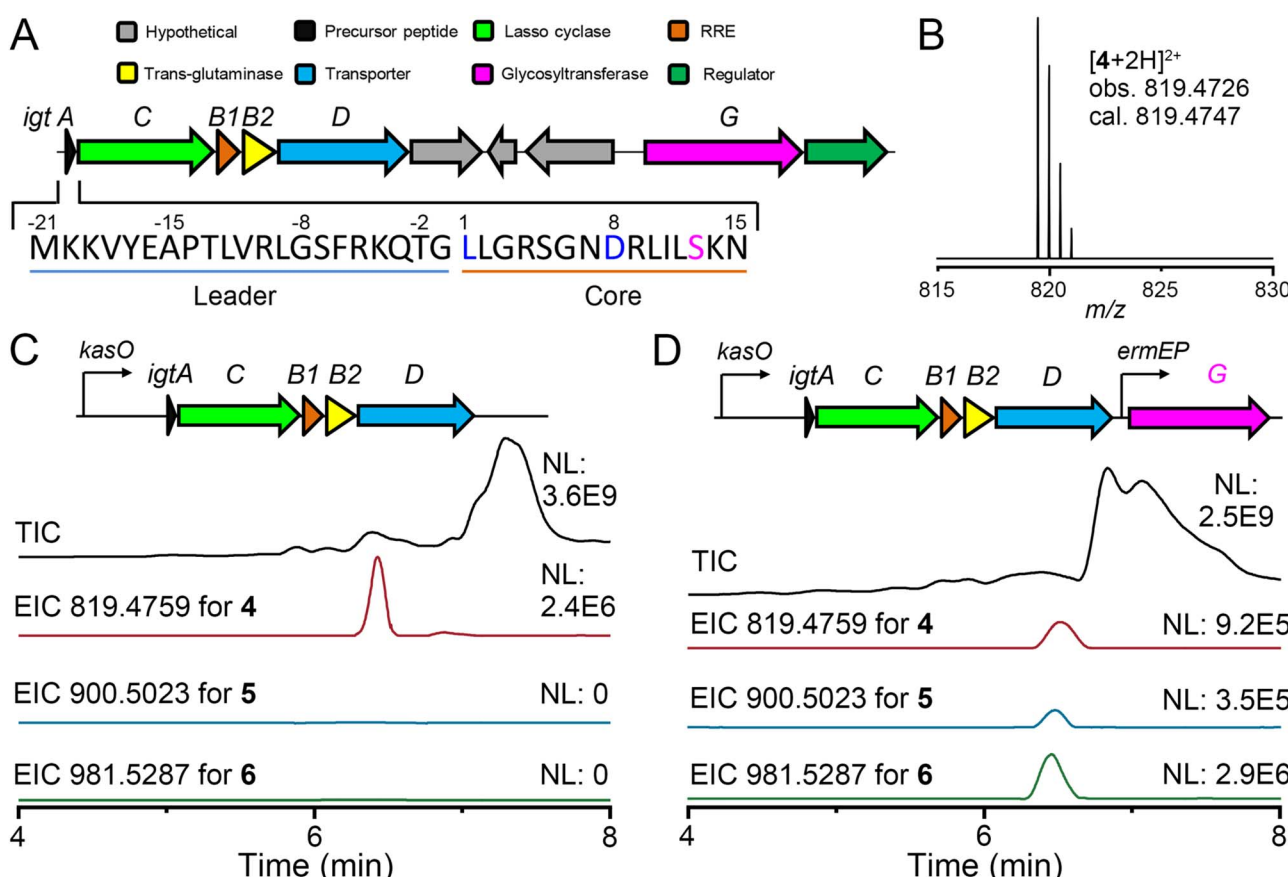


Fig. 3 Correlation of the *igt* BGC with glycosylated lasso peptides from *S. davaonensis* JCM 4913. (A) Organization of *igt* BGC and the sequence of IgtA. (B) The HRMS spectrum of **4** in the extract of *S. davaonensis* JCM 4913. (C and D) Heterologous expression of *igtABCD* (C) and *igtABCDG* (D) in *S. lividans* LJ1018.



fragments under identical conditions (Fig. 3C and D).³⁸ The *igtABCD* fragment was cloned into a pSET-kasO vector under the control of a strong *kasO* promoter.^{38–40} Downstream of the *igtABCD* sequence, an *ermEP* promoter driving the *igtG* gene was inserted. These constructs were individually transformed into *E. coli* ET12567 (pUZ8002) and introduced into *Streptomyces* hosts via *E. coli*/*Streptomyces* conjugation (Tables S6 and 7†). Following extensive screening of host strains and culture media, successful expression of the *igt* BGC was achieved in *S. lividans* LJ1018 and GX28 (ref. 41) using PTM medium. The resulting metabolites were analyzed via LC-HRMS to detect **1–3** and their derivatives with Arg9 (**4–6**).

Cultures expressing only the *igtABCD* genes in LJ1018 and GX28 produced **4**, but not **5** and **6** (Fig. 3C and S22A†). In contrast, strains expressing *igtABCDG* produced both **4** and the glycosylated lasso peptides **5** and **6** (Fig. 3D and S22B†). These results strongly indicate that IgtG functions as a biocatalyst for iterative glycosylation in lasso peptide biosynthesis, a role not previously reported for GTs.

The C-terminal GT domain of IgtG contains a conserved DXD motif (DAD at positions 418–420), commonly associated with catalytic activity in various GTs, potentially by facilitating binding of sugar donors such as UDP-glucose.⁴² To evaluate the functional importance of this motif, site-directed mutations were introduced to replace the Asp residues (D418A, D420A, and D18A/D420A) in heterologous expression systems. LC-HRMS analysis revealed that all mutant strains (LJ1018-*igtABCDG* and GX28-*igtABCDG*) produced only **4** without glycosylation (Fig. S23†), demonstrating the essential role of the DXD motif in IgtG-mediated glycosylation.

IgtG is an iterative GT on the lasso peptide *in vitro*

Heterologous expression experiments could not exclude the possibility that IgtG acts on linear IgtA as a substrate to produce mono-, di- or polyglycosylated peptides, which subsequently undergo lasso structure formation. To investigate whether IgtG recognizes the leader peptide of IgtA, AlphaFold-Multimer⁴³ was utilized to model the IgtG–IgtA complex structure and explore their potential binding interactions (Fig. S24†). The resulting model positioned the DAD motif within a deep cavity of the GT domain, while IgtA was mapped to the surface of the GT domain. The significant spatial separation between IgtA and the catalytic motif of IgtG contradicted the hypothesis that IgtA serves as the glycosylation substrate for IgtG.

Given the nature of IgtG as a membrane protein (Fig. S20†), its two soluble domains, excluding transmembrane helices, were initially cloned into various expression vectors with different fusion tags for protein production and purification in *E. coli*. However, no soluble protein was obtained under any tested conditions for *in vitro* enzymatic reconstitution. Consequently, full-length IgtG was expressed in *S. lividans* GX28 using the pSET-kasO vector. Microsomes containing IgtG were isolated and incubated with various peptides and sugar donors. When IgtG microsomes were incubated with IgtA, UDP-D-glucose, CaCl_2 , and other necessary cofactors, the resulting mass spectra revealed no glycosylated peptides (Fig. 4A). These

findings excluded linear IgtA as a substrate for IgtG, supporting the hypothesis that IgtG acts on lasso peptide **1** during the late stage of the biosynthesis of **3**.

To confirm this, similar *in vitro* reactions were performed using lasso peptide **1** as the substrate instead of IgtA. LC-HRMS analysis of these reactions revealed a new peak corresponding to a product with a yield of 20.2%, determined by the EIC peak area, with a mass identical to **3** (Fig. 4B). Control reactions using GX28 microsomes did not produce **3**. These successful *in vitro* results demonstrate that IgtG catalyzes iterative glycosylation of the mature lasso peptide rather than the linear precursor.

The substrate preferences of IgtG for sugar donors and metal ions were subsequently evaluated (Fig. S25†). Reactions with UDP-L-rhamnose, GDP- α -D-mannose, or UDP- α -D-N-acetylglucosamine as sugar donors in place of UDP-D-glucose resulted in either undetectable levels or yields of less than 1.0% for **3**. Additionally, replacing Ca^{2+} with Mn^{2+} , Zn^{2+} , or Mg^{2+} ions led to reduced production of **3**, with turnover rates of 9.7%, 7.6%, and near 0%, respectively. These findings indicate that IgtG preferentially utilizes glucose as the sugar donor and Ca^{2+} as the metal ion cofactor.

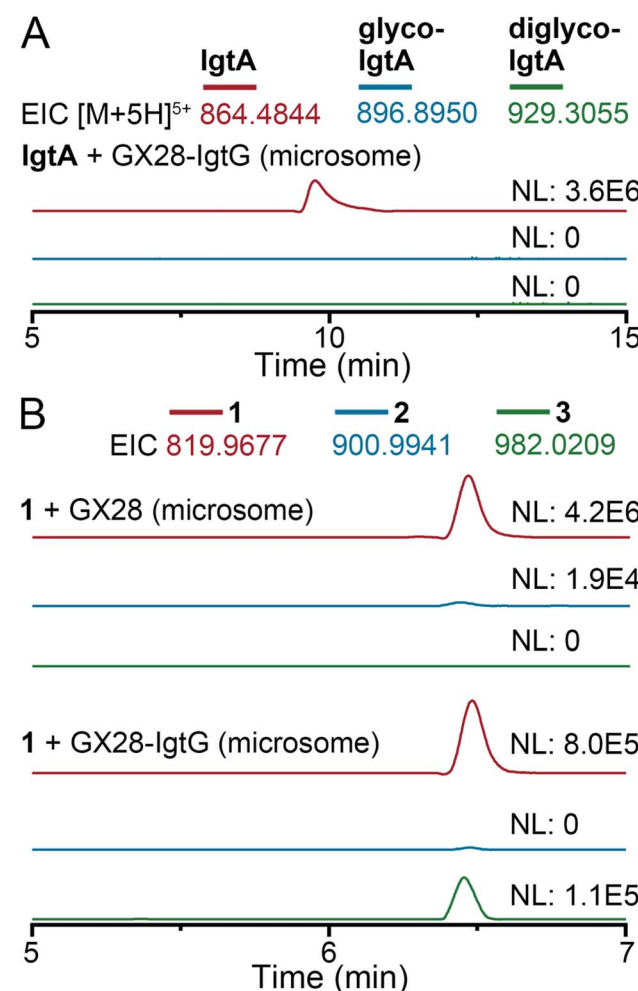


Fig. 4 *In vitro* reconstitution of IgtG. LC-HRMS analysis of IgtG reactions using linear precursor peptide IgtA (A) or lasso peptide **1** (B) as substrates.



IgtG-like GTs are distinct from known RiPP GTs

Given the unique role of IgtG in iterative glycosylation of lasso peptides, a sequence similarity network (SSN) using the IgtG sequence as the query was constructed *via* the Enzyme Function Initiative Enzyme Similarity Tool (EFI-EST).^{44,45} A 72% sequence identity threshold was applied to the SSN to separate IgtG-containing cluster from others (Fig. S26†). The network was further analyzed with the EFI Genome Neighborhood Tool (EFI-GNT) to retrieve co-occurring genes associated with each IgtG-like sequence.

Analysis revealed that IgtG is the sole GT in the lasso peptide BGC. Additionally, an IgtG homolog in *S. iranensis* was found co-occurring with genes encoding a precursor peptide and RimK ATP-grasp ligase, which are core biosynthetic genes of another RiPP class, grasperptides.⁴ The BGC, hereafter referred to as *sir*, also contained genes for a protein-L-isoaspartate O-methyltransferase (PIMT) and a FAD-binding monooxygenase. PIMT-containing grasperptide BGCs have been previously bioinformatically identified⁴⁶ and biochemically characterized.⁴⁷ A BlastP search of the RimK ATP-grasp ligase (SirD) identified 24 similar grasperptide BGCs encoding IgtG-like GTs (SirGs) with over 89% sequence identity (Fig. S27 and Table S8†). A total of 14 non-redundant precursor peptides were identified from these grasperptide BGCs, which are highly conserved across their entire sequences (Fig. S28†). The C-terminal region of these SirAs contains 7–8 Glu/Asp and 6–8 Ser/Thr/Lys residues, which may serve as potential reaction sites for SirDs. The precursor peptide of fuscimiditide, ThfA, contains a PDGQ motif, where the Asp residue is modified into aspartimide by the action of the PIMT ThfM.⁴⁷ A similar PDG

motif was observed in these SirAs, suggesting a potential site for aspartimidation. In addition to Ser/Thr/Lys, two Tyr residues were also observed, which could serve as potential glycosylation sites. No Cys residues were observed in these grasperptide precursors, although Cys residues are known to be glycosylation sites in the biosynthesis of glycocins. The bioinformatic analysis supports the involvement of SirGs in glycosylated grasperptide biosynthesis.

To explore the sequence divergence among RiPP GTs, IgtG and these putative grasperptide GTs were compared with GTs involved in other known RiPP biosynthetic pathways (Fig. 1A–D). A maximum likelihood (ML) phylogenetic tree (Fig. 5) revealed that RiPP GTs generally cluster into distinct clades corresponding to their substrate classes. For instance, thiopeptide and glycocin GTs formed separate clusters, while lanthipeptide GTs were interspersed. Notably, IgtG-like GTs formed a distinct clade, separate from other RiPP GTs, suggesting a unique sequence-function space for their iterative glycosylation roles in lasso peptides and grasperptides.

Conclusions

In summary, we discovered and characterized a novel group of glycosylated lasso peptides, named davasins, which exhibit 0 to 4 glycosylation modifications. Structural elucidation revealed that the polyglycosylation occurs *via* 1,3-glycosidic linkages attached to the side chain hydroxy group of a single Ser residue.

To elucidate the biosynthetic mechanism underlying the iterative glycosylation of ribosomal peptides, genome mining, heterologous expression, and *in vitro* enzymatic assays were performed. The results demonstrate that the GT IgtG, encoded within the *igt* BGC of davasins, specifically modifies the mature lasso peptide rather than the linear precursor peptide. This establishes IgtG as the first PTM enzyme known to iteratively glycosylate mature lasso peptides. In contrast, another type of iterative PTM enzyme acting on lasso peptides belongs to the GCN5-related *N*-acetyltransferase (GNAT) family, which installs two acetyl groups on distinct Lys residues, employing a catalytic pattern distinct from that of IgtG.

Bioinformatic analysis revealed that IgtG is the sole GT co-occurring with lasso peptide biosynthetic genes. However, 24 IgtG-like GTs were identified in the GCs of grasperptides, another class of macrocyclic RiPPs. Phylogenetic analysis confirmed that IgtG-like GTs are evolutionarily distinct, consistent with the unique function of IgtG.

Nature employs a limited set of leader-dependent and leader-independent PTM enzymes in a coordinated manner during RiPP biosynthesis, achieving remarkable structural diversity. As more PTM enzymes capable of directly modifying mature lasso peptides are characterized, it may soon become feasible to design and biosynthesize lasso peptides with tailored structural modifications using combinatorial approaches.

Data availability

The data that support the findings of this study are available within the main text and its ESI files.† Data are also available from the corresponding author upon request.

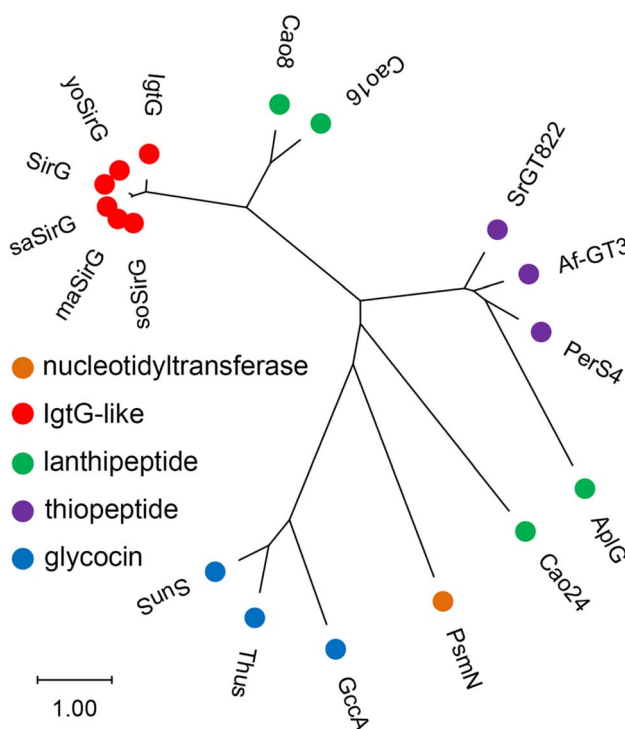


Fig. 5 The ML tree of RiPP GTs. The colorful solid circles are used to indicate GTs with different functions or substrates. The sequences of GTs are listed in Table S9.†



Author contributions

S.-H. Dong conceived the study, supervised the project, and wrote the manuscript with input from all authors. K. Sun conducted the lasso peptide discovery and biochemical experiments, while J.-J. Cui analyzed the data. W. Zhai and X. Lei acquired the NMR spectra. X. Su, Y.-C. Liu, L. Ning, and J. Xiong contributed to the experimental work. S. Luo and K. Gao participated in discussions.

Conflicts of interest

The authors declare no competing financial interest.

Acknowledgements

This work was supported by the National Natural Science Foundation of China (no. 22377046, 22077056, 22107040, 22477050, and 21907046) and the Science and Technology Major Program of Gansu Province of China (22ZD6FA006, 23ZDFA015, and 24ZD13FA017).

References

- 1 D. Chettri, M. Chirania, D. Boro and A. K. Verma, *Life Sci.*, 2024, **348**, 122689.
- 2 K. T. Schjoldager, Y. Narimatsu, H. J. Joshi and H. Clausen, *Nat. Rev. Mol. Cell Biol.*, 2020, **21**, 729–749.
- 3 P. G. Arnison, M. J. Bibb, G. Bierbaum, A. A. Bowers, T. S. Bugni, G. Bulaj, J. A. Camarero, D. J. Campopiano, G. L. Challis, J. Clardy, P. D. Cotter, D. J. Craik, M. Dawson, E. Dittmann, S. Donadio, P. C. Dorrestein, K. D. Entian, M. A. Fischbach, J. S. Garavelli, U. Goransson, C. W. Gruber, D. H. Haft, T. K. Hemscheidt, C. Hertweck, C. Hill, A. R. Horswill, M. Jaspars, W. L. Kelly, J. P. Klinman, O. P. Kuipers, A. J. Link, W. Liu, M. A. Marahiel, D. A. Mitchell, G. N. Moll, B. S. Moore, R. Muller, S. K. Nair, I. F. Nes, G. E. Norris, B. M. Olivera, H. Onaka, M. L. Patchett, J. Piel, M. J. Reaney, S. Rebuffat, R. P. Ross, H. G. Sahl, E. W. Schmidt, M. E. Selsted, K. Severinov, B. Shen, K. Sivonen, L. Smith, T. Stein, R. D. Sussmuth, J. R. Tagg, G. L. Tang, A. W. Truman, J. C. Vederas, C. T. Walsh, J. D. Walton, S. C. Wenzel, J. M. Willey and W. A. van der Donk, *Nat. Prod. Rep.*, 2013, **30**, 108–160.
- 4 M. Montalban-Lopez, T. A. Scott, S. Ramesh, I. R. Rahman, A. J. van Heel, J. H. Viel, V. Bandarian, E. Dittmann, O. Genilloud, Y. Goto, M. J. Grande Burgos, C. Hill, S. Kim, J. Koehnke, J. A. Latham, A. J. Link, B. Martinez, S. K. Nair, Y. Nicolet, S. Rebuffat, H. G. Sahl, D. Sareen, E. W. Schmidt, L. Schmitt, K. Severinov, R. D. Sussmuth, A. W. Truman, H. Wang, J. K. Weng, G. P. van Wezel, Q. Zhang, J. Zhong, J. Piel, D. A. Mitchell, O. P. Kuipers and W. A. van der Donk, *Nat. Prod. Rep.*, 2021, **38**, 130–239.
- 5 S. Ahlawat, B. N. Shukla, V. Singh, Y. Sharma, P. Choudhary and A. Rao, *Biotechnol. Adv.*, 2024, **75**, 108415.
- 6 P. T. Northcote, M. Siegel, D. B. Borders and M. D. Lee, *J. Antibiot.*, 1994, **47**, 901–908.
- 7 Y. Dashti, F. Mohammadipanah, Y. Zhang, P. M. Cerqueira Diaz, A. Vocat, D. Zabala, C. D. Fage, I. Romero-Canelon, B. Bunk, C. Sproer, L. M. Alkhafaf, J. Overmann, S. T. Cole and G. L. Challis, *ACS Infect. Dis.*, 2024, **10**, 3378–3391.
- 8 Y. Ding, Y. Yu, H. Pan, H. Guo, Y. Li and W. Liu, *Mol. Biosyst.*, 2010, **6**, 1180–1185.
- 9 C. Zhang, J. Occi, P. Masurekar, J. F. Barrett, D. L. Zink, S. Smith, R. Onishi, S. Ha, O. Salazar, O. Genilloud, A. Basilio, F. Vicente, C. Gill, E. J. Hickey, K. Dorso, M. Motyl and S. B. Singh, *J. Am. Chem. Soc.*, 2008, **130**, 12102–12110.
- 10 J. E. Leet, W. Li, H. A. Ax, J. A. Matson, S. Huang, R. Huang, J. L. Cantone, D. Drexler, R. A. Dalterio and K. S. Lam, *J. Antibiot.*, 2003, **56**, 232–242.
- 11 T. Sasaki, T. Otani, H. Matsumoto, N. Unemi, M. Hamada, T. Takeuchi and M. Hori, *J. Antibiot.*, 1998, **51**, 715–721.
- 12 A. Regueiro-Ren and Y. Ueda, *J. Org. Chem.*, 2002, **67**, 8699–8702.
- 13 Y. Du, Y. Xia, L. Wu, L. Chen, J. Rong, J. Fan, Y. Chen and X. Wu, *Microb. Biotechnol.*, 2024, **17**, e14412.
- 14 M. Iorio, O. Sasso, S. I. Maffioli, R. Bertorelli, P. Monciardini, M. Sosio, F. Bonezzi, M. Summa, C. Brunati, R. Bordoni, G. Corti, G. Tarozzo, D. Piomelli, A. Reggiani and S. Donadio, *ACS Chem. Biol.*, 2014, **9**, 398–404.
- 15 F. J. Ortiz-Lopez, D. Carretero-Molina, M. Sanchez-Hidalgo, J. Martin, I. Gonzalez, F. Roman-Hurtado, M. de la Cruz, S. Garcia-Fernandez, F. Reyes, J. P. Deisinger, A. Muller, T. Schneider and O. Genilloud, *Angew. Chem. Int. Ed. Engl.*, 2020, **59**, 12654–12658.
- 16 T. Zyubko, M. Serebryakova, J. Andreeva, M. Metelev, G. Lippens, S. Dubiley and K. Severinov, *Chem. Sci.*, 2019, **10**, 9699–9707.
- 17 L. L. Lairson, B. Henrissat, G. J. Davies and S. G. Withers, *Annu. Rev. Biochem.*, 2008, **77**, 521–555.
- 18 D. Fujinami, C. V. Garcia de Gonzalo, S. Biswas, Y. Hao, H. Wang, N. Garg, T. Lukk, S. K. Nair and W. A. van der Donk, *Cell Chem. Biol.*, 2021, **28**, 1740–1749.
- 19 B. J. Drummond, T. S. Loo, M. L. Patchett and G. E. Norris, *J. Bacteriol.*, 2021, **203**, e00529–e00520.
- 20 R. Nagar and A. Rao, *Glycobiology*, 2017, **27**, 766–776.
- 21 J. Stepper, S. Shastri, T. S. Loo, J. C. Preston, P. Novak, P. Man, C. H. Moore, V. Havlicek, M. L. Patchett and G. E. Norris, *FEBS Lett.*, 2011, **585**, 645–650.
- 22 H. Venugopal, P. J. Edwards, M. Schwalbe, J. K. Claridge, D. S. Libich, J. Stepper, T. Loo, M. L. Patchett, G. E. Norris and S. M. Pascal, *Biochemistry*, 2011, **50**, 2748–2755.
- 23 H. Wang, T. J. Oman, R. Zhang, C. V. Garcia De Gonzalo, Q. Zhang and W. A. van der Donk, *J. Am. Chem. Soc.*, 2014, **136**, 84–87.
- 24 W. Sheng, B. Xu, S. Chen, Y. Li, B. Liu and H. Wang, *Org. Biomol. Chem.*, 2020, **18**, 6095–6099.
- 25 F. Roman-Hurtado, M. Sanchez-Hidalgo, J. Martin, F. J. Ortiz-Lopez and O. Genilloud, *Antibiotics*, 2021, **10**.
- 26 Y. Duan, W. Niu, L. Pang, X. Bian, Y. Zhang and G. Zhong, *Int. J. Mol. Sci.*, 2022, **23**, 7231–7247.



27 L. Cao, M. Beiser, J. D. Koos, M. Orlova, H. E. Elashal, H. V. Schroder and A. J. Link, *J. Am. Chem. Soc.*, 2021, **143**, 11690–11702.

28 L. Cao, H. E. Elashal and A. J. Link, *Biochemistry*, 2023, **62**, 695–699.

29 J. Xiong, S. Wu, Z.-Q. Liang, S. Fang, F.-Y. Tao, X.-T. Gong, Q. Wu, J.-J. Cui, K. Gao, S. Luo, D. Lei and S.-H. Dong, *bioRxiv*, 2025, preprint, DOI: [10.1101/2024.12.31.630886](https://doi.org/10.1101/2024.12.31.630886), <https://www.biorxiv.org/content/10.1101/2024.12.31.630886v1>.

30 J. I. Tietz, C. J. Schwalen, P. S. Patel, T. Maxson, P. M. Blair, H. C. Tai, U. I. Zakai and D. A. Mitchell, *Nat. Chem. Biol.*, 2017, **13**, 470–478.

31 L. A. Harris, P. M. B. Saint-Vincent, X. Guo, G. A. Hudson, A. J. DiCaprio, L. Zhu and D. A. Mitchell, *ACS Chem. Biol.*, 2020, **15**, 3167–3175.

32 I. M. Sims, S. M. Carnachan, T. J. Bell and S. F. R. Hinkley, *Carbohydr. Polym.*, 2018, **188**, 1–7.

33 T. Tanaka, T. Nakashima, T. Ueda, K. Tomii and I. Kouno, *Chem. Pharm. Bull.*, 2007, **55**, 899–901.

34 K. Blin, S. Shaw, H. E. Augustijn, Z. L. Reitz, F. Biermann, M. Alanjary, A. Fetter, B. R. Terlouw, W. W. Metcalf, E. J. N. Helfrich, G. P. van Wezel, M. H. Medema and T. Weber, *Nucleic Acids Res.*, 2023, **51**, W46–W50.

35 K. Blin, S. Shaw, A. M. Kloosterman, Z. Charlop-Powers, G. P. van Wezel, M. H. Medema and T. Weber, *Nucleic Acids Res.*, 2021, **49**, W29–W35.

36 J. Hallgren, K. D. Tsirigos, M. D. Pedersen, J. J. Almagro Armenteros, P. Marcatili, H. Nielsen, A. Krogh and O. Winther, *bioRxiv*, 2022, preprint, DOI: [10.1101/2022.04.08.487609](https://doi.org/10.1101/2022.04.08.487609), <https://www.biorxiv.org/content/10.1101/2022.04.08.487609v1>.

37 H. Li, W. Li, K. Song, Y. Liu, G. Zhao and Y. L. Du, *Synth. Syst. Biotechnol.*, 2024, **9**, 127–133.

38 M. X. Guo, M. M. Zhang, K. Sun, J. J. Cui, Y. C. Liu, K. Gao, S. H. Dong and S. Luo, *J. Nat. Prod.*, 2023, **86**, 2333–2341.

39 W. Wang, X. Li, J. Wang, S. Xiang, X. Feng and K. Yang, *Appl. Environ. Microbiol.*, 2013, **79**, 4484–4492.

40 G. Pan, Z. Xu, Z. Guo, Hindra, M. Ma, D. Yang, H. Zhou, Y. Gansemans, X. Zhu, Y. Huang, L. X. Zhao, Y. Jiang, J. Cheng, F. Van Nieuwerburgh, J. W. Suh, Y. Duan and B. Shen, *Proc. Natl. Acad. Sci. U. S. A.*, 2017, **114**, E11131–E11140.

41 Q. Peng, G. Gao, J. Lu, Q. Long, X. Chen, F. Zhang, M. Xu, K. Liu, Y. Wang, Z. Deng, Z. Li and M. Tao, *Front. Microbiol.*, 2018, **9**, 3042.

42 I. M. Saxena, R. M. Brown Jr and T. Dandekar, *Phytochemistry*, 2001, **57**, 1135–1148.

43 M. Mirdita, K. Schutze, Y. Moriwaki, L. Heo, S. Ovchinnikov and M. Steinegger, *Nat. Methods*, 2022, **19**, 679–682.

44 N. Oberg, R. Zallot and J. A. Gerlt, *J. Mol. Biol.*, 2023, **435**, 168018.

45 R. Zallot, N. Oberg and J. A. Gerlt, *Biochemistry*, 2019, **58**, 4169–4182.

46 S. Ramesh, X. Guo, A. J. DiCaprio, A. M. De Lio, L. A. Harris, B. L. Kille, T. V. Pogorelov and D. A. Mitchell, *ACS Chem. Biol.*, 2021, **16**, 2787–2797.

47 H. E. Elashal, J. D. Koos, W. L. Cheung-Lee, B. Choi, L. Cao, M. A. Richardson, H. L. White and A. J. Link, *Nat. Chem.*, 2022, **14**, 1325–1334.

